Deployment feasibility studies of variable buoyancy anchors for floating wind applications *

Rodrigo Martinez[1], Sergi Arnau[1], Callum Scullion[2], Paddy Collins[2], Richard D. Neilson[1], and Marcin Kapitaniak[1]

[1] The National Decommissioning Centre, School of Engineering, University of Aberdeen, UK
[2] Aubin Group, Castle Street, Castlepark Industrial Estate, Ellon AB41 9RF, UK

Abstract. To study the feasibility of deploying a novel type of anchor with variable buoyancy for mooring floating offshore wind turbines, a set of detailed modelling studies was performed in the state-of-the-art, Marine Simulator at the National Decommissioning Centre (NDC). The aim of the multi-physics simulations is to fully assess the proposed deployment method using a small tugboat fitted with a simple winch, thereby simplifying the process and reducing installation costs. The anchor has a 10 m square base, 4.5 m height and weight of 163 tonnes. The anchor is subjected to irregular waves with a JONSWAP spectrum with a significant wave height up to 5 m and peak period of 10 s. The analysis is divided in three sections: characterisation of the anchor buoyancy, positioning the anchor under the stern of the vessel and the controlled descent of the anchor to the seabed. An ideal winch speed of 0.35 m/s is identified, at which working load range on the winch cable decreases from 80 kN at the lowest winch speeds to about 30 kN. The sinking trajectory is similar at all winch speeds, however, the slower the descent, the further the anchor drifts. At this winch velocity, the descent from the resting position under the stern to the seabed takes roughly 5 minutes. In addition, the anchor's yaw range during the descent is below 10° at the optimal conditions.

Keywords: Offshore wind · Anchor dynamics · Virtual prototyping.

1 Introduction

The economic drivers for lowering CapEx and OpEx of floating offshore wind technologies calls for innovation. In this study, the feasibility of deploying a novel type of anchor with variable buoyancy for mooring floating offshore wind turbines is presented. A set of detailed modelling studies are performed it the state-of-the-art, Marine Simulator at the National Decommissioning Centre (NDC). Using the multi-physics simulation allows for a more economical proof-of-concept

* Supported by EPSRC Supergen ORE Hub, ORE Catapult, FOW CoE, Aubin Group, Net Zero Technology Centre, The University of Aberdeen, Oceanetics Inc.

approach, that will allow to fully assess the proposed deployment method and de-risk future offshore deployment. By using the proposed floating anchor, the use of heavy-lifting cranes and vessels could potentially be avoided, thereby reducing complexity and associated expenses. Instead, the anchor can be deployed from a smaller vessel, equipped with a simple winch. Once the anchor is towed to the deployment site, the anchor is pumped with liquid ballast and lowered with the winch. The proposed anchor (Figure 1) has the shape of a truncated pyramid with a 10 m square base and is 4.46 m high (eyebolt inclusive). The empty anchor has a weight of 163 tonnes.

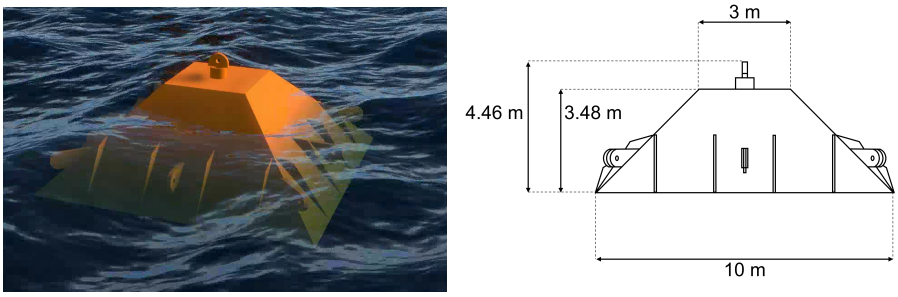

Fig. 1: Left: 3D representation of the anchor in the simulator's environment. Right: 2D diagram of the anchor.

2 Literature review

This section provides an insight to the current state of the deployment of offshore wind turbines, their moorings and anchors as well as the typical weather conditions in which offshore deployments are performed.

2.1 Floating offshore wind turbines

Offshore wind turbines can be divided in two categories: floating and fixed to the seabed. Much of the offshore wind energy resource worldwide is located over deep water and current fixed-bottom turbine technology may not be an economical solution for developing this deep water resource. Floating offshore wind turbines allow this resource to be harnessed [9]. Floating turbines are classified in four predominant types: semi-submersible, tension-leg-platform (TLP), spar and barge platforms. All of these require anchor(s) to be moored to the seabed. Regardless of the anchor type, deployments are usually proposed using established anchoring technologies/methodologies borrowed from the O&G industry [1]. At the time of writing, no literature was found on the development of novel anchoring technologies despite its potential for improvement [5,8,10].

2.2 Anchor deployment

Little information is found related to the type of anchor employed for floating wind. However, knowledge from the Oil & Gas industry is adapted to meet the offshore wind requirements [4,3]. Figure 2 shows the most common anchors used for floating wind turbines [4]. In comparison with other types of anchors, gravity anchors (d) require medium to hard soils, their main loading direction is vertical but can perform at different angles. A drawback of gravity anchors is the weight for which they rely to work efficiently. This heavy weight increases installation costs and decreases the potential to recover the anchors upon decommissioning. Each type of anchor has its own deployment procedure. Drag-embedded (a) and gravity anchors (d) are simply lowered to the seabed. Whereas driven (b) and suction (c) piles need further interventions for their installation. The selection criteria for anchors is highly dependant on the seabed conditions of the deployment location. Hence, bathymetry surveys should be conducted as part of the planning process.

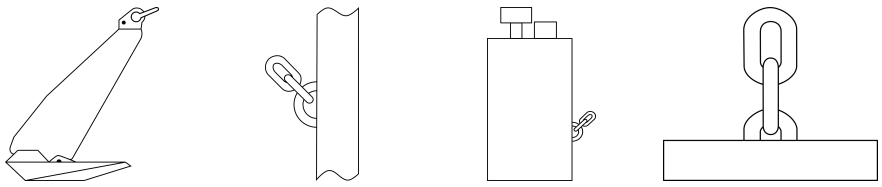

Fig. 2: Anchor types generally used in floating offshore turbines: a) drag-embedded, b) driven pile, c) suction pile, d) gravity anchor. Adapted from [4].

2.3 Flow characteristics and weather window

Offshore deployment is limited by so-called weather windows. These weather windows are characterised by a series of environmental conditions that allow for the safe deployment of equipment [13,6]. The main characteristics associated to weather windows are the significant wave height (H_S) and flow velocity (U). Average flow velocity around the North Sea is usually below 1m/s ($\sim$ 2 kn) [12,2]; however, in certain areas characterised by channels, straits or some other land features, can reach up to 4 m/s ($\sim$ 8 kn)[7,11].

3 Methodology

The proposed 3D anchor CAD model is imported into the OSC simulator software with the adequate collision model. The schematic of the anchor is depicted on Figure 3 (left). The anchor has a base width of 10.00 m, body height of 3.48 m,

overall height of 4.46 m and air weight of 163.20 t. The inertia properties of the steel anchor body are calculated based on the CAD drawing and are imported into the OSC simulator as part of the collision model generation process. Collision model generation is based on creating a mesh structure to represent the anchor and is generated using the software 3DS Max before importing it into the OSC simulator. Due to the simulator only taking into account the volume of the steel plates and internal bulkheads used to create the anchor shape, it is necessary to create a solid part that will represent the inner volume of the anchor (Figure 3 (right)). This inner volume is filled/emptied to modify the anchor's buoyancy. The inner volume is fixed to the anchor within the simulator environment. The model of the anchor is assembled in the OSC simulator with the two components depicted in Figure 3, where the inner volume representing the air/liquid is fixed rigidly inside the anchor. In order to ensure that the anchor floats, the inner volume is assigned a mass of 170 kg, which corresponds to the inner volume of 142.44 m^3 filled with air. The anchor is connected to the hose reel, using a standard 4" hose and a 50 mm OD steel winch cable.

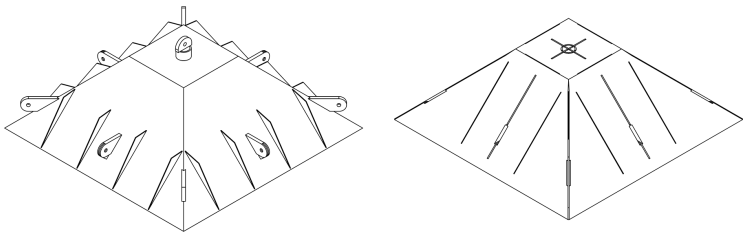

Fig. 3: 3D model of the anchor (left) and the internal representation (right).

The anchor deployment process is shown in Figure 4. The developed scenario assumes that the floating anchor will be towed to the site and deployed from a support vessel equipped with a winch and a hose reel. As shown in Figure 4.1, the floating anchor is connected to the winch using a cable and through a hose to the reel. Through the hose, the ballast fluid is pumped into the anchor. Once the anchor has negative buoyancy, the anchor starts sinking and positions itself under the stern of the vessel, eventually hanging from the winch cable (Figure 4.2). At this point, the anchor starts its controlled descent to the seabed guided by the winch at the desired velocity (Figure 4.3).

The simulation scenario assumes that the anchor is deployed in 100 m water depth with ocean conditions represented by irregular waves with a JONSWAP spectrum with significant wave height of 1 m, current of 0.1 kn and peak period of 10 s. Although the addition of wind is possible in the simulator, it was opted not to include this in the first round of tests.

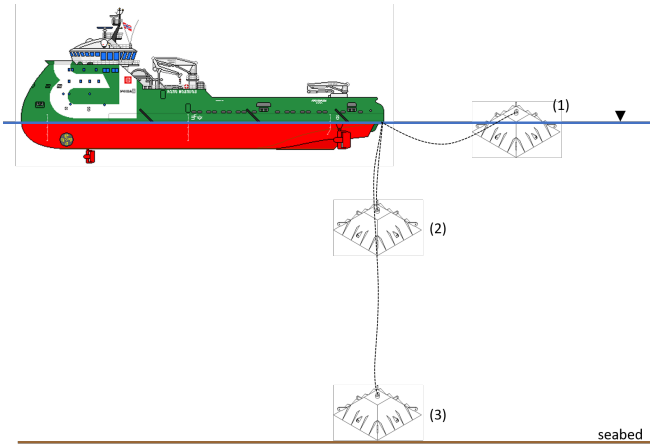

Fig. 4: Schematic of the deployment process of the anchor: (1) initial position of the anchor after towing. Pumping of ballast commences to generate negative buoyancy. (2) positioning of the anchor underneath the vessel's stern. (3) controlled descent of the anchor by means of a simple winch.

4 Results

The analysis of the deployment process is divided in three sections: 1.- characterisation of the anchor's buoyancy, 2.- positioning the anchor under the stern of the vessel by pumping ballast into the anchor to create negative buoyancy and, 3.- the controlled/guided descent of the anchor to the seabed by a winch.

4.1 Buoyancy

To determine the buoyancy limit of the anchor when filled with air, the mass of the anchor is increased until the anchor is fully submerged. The anchor buoyancy characterisation is shown in Figure 5, where each curve corresponds to a specific pump rate. The vertical dashed line corresponds to the actual mass of the anchor (163.2 t), while the two horizontal dashed lines denote the anchor body height (3.48 m) and overall anchor height (4.46 m), respectively. As shown, the buoyancy characteristics of the anchor change when the draft reaches the lower dashed line (167.3 t), which means that the anchor body is fully submerged and only the lifting hook remains above the water level. After this point there is a sharp change in the buoyancy characteristics and the precise buoyancy limit can be determined from the crossing point between the curve and the top horizontal line (lifting hook at the water level). When the anchor mass reaches between 167 and 168 t, depending on the pump rate, the anchor becomes neutrally buoyant. This means that anchor possesses a gross buoyancy of about 4 t. The difference between the different pump rates is attributed to the inertia created by the speed at which the ballast is being pumped.

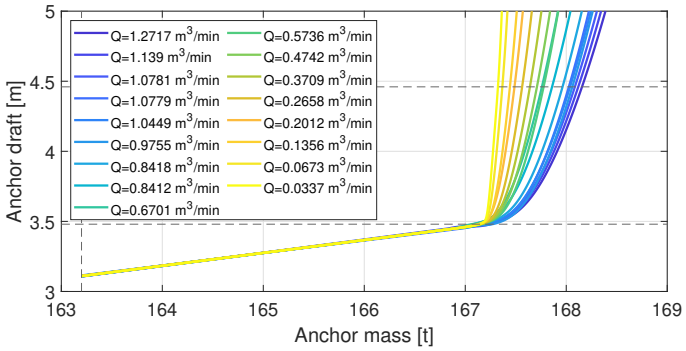

Fig. 5: Anchor buoyancy tests as a function of pump flow rate Q. Vertical line represents the weight of the anchor in air. The bottom horizontal line represent the height of the anchor without eye-bolt, the top line takes into consideration the height of the eye-bolt.

4.2 Positioning

The tests positioning the vessel underneath the vessel stern are analysed as a function of the pump rate Q (m^3/min). The variation of the winch force (F_W), anchor vertical position (Z_A) with the pump rate (Q) are shown in Figure 6 (left). Vertical dashed lines indicate the time at which F_W and Z_A stabilise. At faster pump rates (Q≈1 m^3/min), the anchor can be positioned underneath the stern of the vessel in under 5 minutes. In contrast, at slower pump rates (Q≈0.05 m^3/min), the anchor takes up to 35 minutes to position under the vessel. Due to the length of the cable, the forces acting on the winch cable (F_W) remain constant until the anchor is roughly 18 m under the water surface. The anchor 3D trajectory from the surface to underneath the vessel is shown in Figure 6 (right). At the lowest pump rate, the trajectory presents oscillations compared to the other pump rates. This is thought to be associated to the time it takes for the anchor to reach the bottom of the vessel, making it more susceptible to wave-induced effect.

Comparing the settling times of the winch force and anchor sinking velocity is shown in Figure 7 for all pump rates Q. At Q=0.5 m^3/min, the anchor reaches its position under the stern around 10.5 minutes before the winch force stabilises. This means that once the anchor is in position, the ballast gets pumped for a further 10 minutes. In contrast, at higher Q, the pump stops a couple of minutes before the anchor has reached its position. At Q=0.4 m^3/min, both F_W and Z_A settle in 4.8 minutes. From this point, as pump rate increases, settling times decrease at a lower rate. At Q=1 m^3/min F_W settles in 1.9 minutes and Z_A settles in 2.9 minutes.

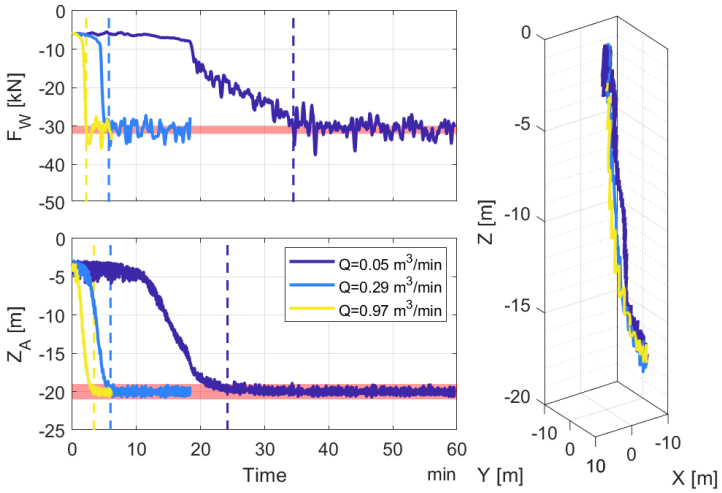

Fig. 6: Winch force (top) and anchor vertical position (bottom) for Q=0.05, 0.29 and 0.97 m^3/min. Vertical dashed lines represent the time at which the signals stabilise.

4.3 Descent

In contrast to the positioning tests, the anchor descent tests are analysed as a function of the winch velocity V_W (m/s). In the preliminary results, a range of winch velocities, associated forces acting on the winch cable, along with the three-dimensional anchor descent trajectories and orientation are carefully analysed. Results from Figure 8 (left) indicate that, in the presence of passive heave compensation, the working load amplitude on the winch cable decreases from 80 kN at the lowest winch velocities to about 30 kN for winch velocities above 0.35 m/s. The spread visible in the force data is associated to the wave-induced

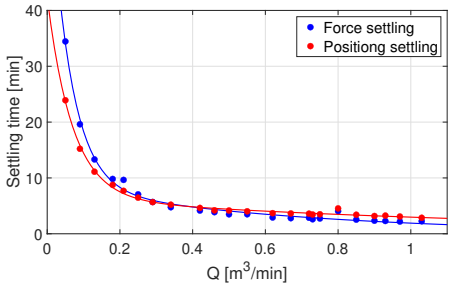

Fig. 7: Variation of winch force (top) and anchor positioning (bottom) settling time with pump rate Q. Exponential curves fitted.

heave oscillations of the anchor and the vessel. Similar behaviour can be seen in Figure 8 (right), where the deployment time stabilises above 0.35 m/s.

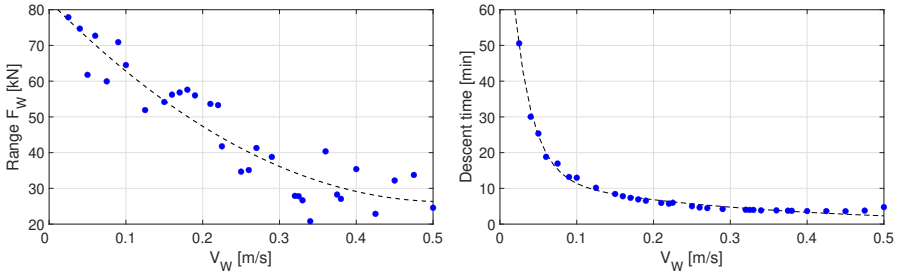

Fig. 8: Winch force range (left) and descent time (right) as a function of winch velocity.

The sinking trajectory is shown in Figure 9 (centre). The trajectory is similar at all winch velocities. However, the slower the descent, the further the anchor drifts from its initial position (up to 10 m in the Y direction). As seen in Figure 9 (bottom-left), at winch velocities above 3.5 m/s, the descent from the resting position under the vessel stern to the seabed takes under 5 minutes and the oscillations on the loading signal associated to the wave movement of the vessel is no longer an issue. The orientation range of the anchor is shown in Figure 9 (right). The yaw range is the difference between the yaw angle at the time the anchor reaches the seabed and the angle the winch is released. For pitch and roll, which are only influenced by the waves, the range is the difference between the maximum and minimum values in the time series. During the anchor's descent, roll is kept almost constant at all winch velocities, with a standard deviation of 0.6°. Pitch has more variation as winch velocity increases, with a standard deviation of 1.7°. However, in the considered range of winch velocities, the anchor's rotation about its vertical axis (yaw) presents a standard deviation of 10°.

In Figure 10 (left), the anchor descent velocity is plotted against winch velocities considered. It can be seen that for V_W values below 0.35 m/s the anchor descent is governed by the winch. However, at higher V_W values, the anchor reaches an equilibrium and it's descent velocity does not increase (free fall), regardless of the winch velocity.

Preliminary results using more ballast to sink the anchor are shown in Figure 10 (centre/right). It appears that all weights take the same amount of time (4 minutes). However, this is explained looking at the winch force time series, where the tension in the cable increases with weight and the wave-induced oscillations are more visible. These oscillations have the same amplitude for all ballast weights. This means that for each anchor weight, there will be a case-specific winch speed at which descent speed and winch speed are the same (Figure 10 (left)).

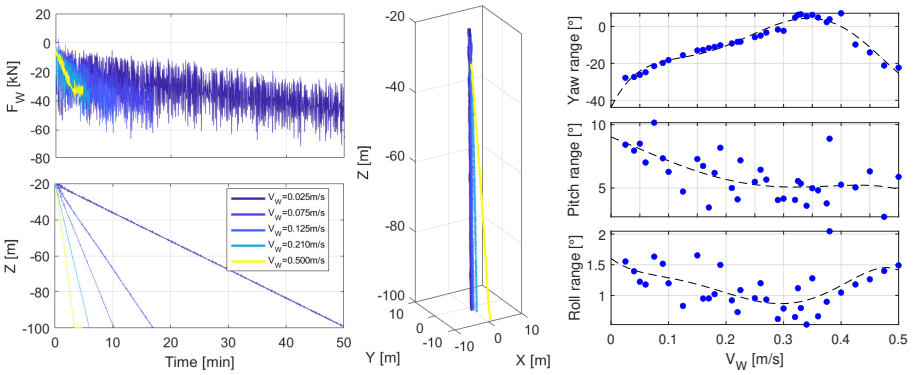

Fig. 9: Winch force range (top-left) and descent time (bottom-left) as a function of winch velocity and 3D descent trajectory (centre). Ranges of angular displacements of the anchor in yaw, pitch and roll directions (right).

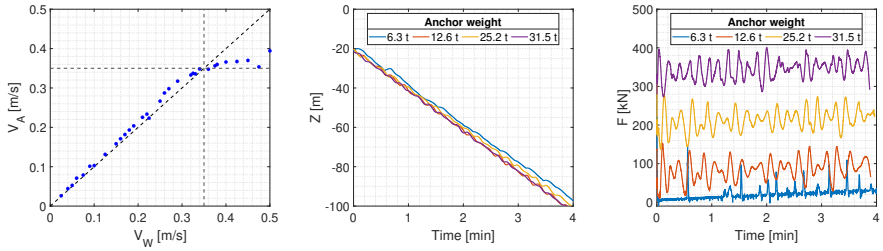

Fig. 10: Left: Variation of the anchor deployment speed (V_A) with the winch speed (V_W). Centre: Vertical position of anchors with different ballast weights. Right: Winch force (F_W) for different anchor ballast weights.

5 Conclusions

The deployment of a novel anchor design using a real-physics simulator is described in this work. The anchor's variable buoyancy means that it can float and be towed to the deployment site. This also allows for the deployment to be done by means of a simple winch.

Having established the anchor buoyancy limit (approximately 4 tonnes), we were able to study the effect of ballast pumping rate on the first deployment step (positioning under the stern). The rate at which the ballast is pumped into the anchor has a direct impact on the time it takes for the anchor to position itself under the stern of the vessel, at about 20 m depth. At Q$\approx$ 1 m^3/min the anchor reaches the position in under 5 minutes, however, at the lowest Q values, it takes up to 25 minutes.

The analysis performed on the anchor dynamics during its descent, indicates that a winch velocity of 0.35 m/s is the best in this scenario as the anchor is

allowed to descend almost at free-fall whilst still being controlled by the winch. At this winch velocity, the forces acting on the winch have a working range of 30 kN.

References

1. Bjerkseter, C., Agotnes, A.: Levelised costs of energy for offshore floating wind turbine concepts. Master's thesis, Norwegian University of Life Sciences, Department of Mathematical Sciences and Technology (2013)
2. Davies, A.M., Furnes, G.K.: Observed and computed m2 tidal currents in the north sea. Journal of Physical Oceanography **10**, 237–257 (1980)
3. Ikhennicheu, M., Lynch, M., Doole, S., Borisade, F., Matha, D., Dominguez, J.L., Vicente, R.D., Habekost, T., Ramirez, L., Potestio, S., Molins, C., Trubat, P.: D2.1 - review of the state of the art of mooring and anchoring designs, technical challenges and identification of relevant dlcs. Tech. rep., WindEurope & IREC (2020)
4. James, R., Ros, M.C.: Floating offshore wind: Market and technology review. Tech. rep., The Carbon Trust (2015)
5. James, R., Weng, W.Y., Spradbery, C., Jones, J., Matha, D., Mitzlaff, A., Ahilan, R.V., Frampton, M., Lopes, M.: Floating Wind Joint Industry Project - Phase I Summary Report. Tech. rep., The Carbon Trust (2018)
6. O'Connor, M., Lewis, T., Dalton, G.: Weather window analysis of irish west coast wave data with relevance to operations & maintenance of marine renewables. Renewable Energy **52**, 57–66 (2013)
7. Sellar, B., Wakelam, G.: Characterisation of tidal flows at the European Marine Energy Centre in the absence of ocean waves. Energies **11**(1), 176 (2018)
8. Spearman, D.K., Strivens, S., Matha, D., Cosack, N., Macleay, A., Regelink, J., Patel, D., Walsh, T.: Floating Wind Joint Industry Project - Phase II Summary Report. Tech. rep., The Carbon Trust (2020)
9. Stewart, G., Muskulus, M.: A review and comparison of floating offshore wind turbine model experiments. Energy Procedia **94**, 227–231 (2016), 13th Deep Sea Offshore Wind R&D Conference, EERA DeepWind 2016
10. Strivens, S., Northridge, E., Evans, H., Harvey, M., Camp, T., Terry, N.: Floating Wind Joint Industry Project - Phase III Summary Report. Tech. rep., The Carbon Trust (2021)
11. Sutherland, D.R.J., Sellar, B.G., Harding, S., Bryden, I.: Initial flow characterisation utilising turbine and seabed installed acoustic sensor arrays. In: Proceedings of the 10th European Wave and Tidal Energy Conference. pp. 1–8. Aalborg (2013)
12. Vindenes, H., Orvik, K.A., Søiland, H., Wehde, H.: Analysis of tidal currents in the north sea from shipboard acoustic doppler current profiler data. Continental Shelf Research **162**, 1–12 (2018)
13. Walker, R.T., Nieuwkoop-Mccall, J.V., Johanning, L., Parkinson, R.J.: Calculating weather windows: Application to transit, installation and the implications on deployment success. Ocean Engineering **68**, 88–101 (2013)